Data Supplement for McHugo et al., Hyperactivity and Reduced Activation of Anterior Hippocampus in Early Psychosis. Am J Psychiatry (doi: 10.1176/appi.ajp.2019.19020151)

Supplementary Methods

Inclusion criteria

Psychiatric diagnoses were assessed with the Structured Clinical Interview for DSM-IV, TR (SCID) (1). Clinical symptoms at the time of scanning were characterized using the Positive and Negative Symptom Scale (PANSS (2)). Inclusion criteria for patients required a diagnosis of schizophreniform disorder, schizophrenia, or schizoaffective disorder, with a duration of psychosis less than 2 years. Duration of psychosis and prodrome were determined through SCID interview, medical record review, and the Symptom Onset in Schizophrenia Inventory (SOS (3)), a measure for rating prodromal versus psychotic symptoms. Chlorpromazine equivalents (N=43) were calculated using the formulas from Gardner et al. (4). Healthy control participants were recruited on the basis of demographic matching to the patient sample (age, gender, race, and parental education) and had no past or present psychiatric diagnoses as confirmed by the SCID. Smoking status was assessed through self-report of current use of tobacco products including cigarettes, cigars, chewing tobacco, etc.

Exclusionary criteria for all participants included the presence of significant head injury, major medical illnesses, pregnancy, pre-morbid IQ less than 70 as estimated by the Wechsler Test of Adult Reading (WTAR, (5)) and current substance abuse or dependence within the past month at the time of study enrollment. Two healthy control participants were excluded for poor

performance on the task (hit rate < 50% in at least 1 condition); no participants were excluded for excessive false alarms rates (all participant false alarm rates <= 25%). Eight patients were excluded for gross motion (6 with greater than 6mm or 4 degrees of motion; 2 for motion on structural). Five participants were excluded for incomplete fMRI coverage of the hippocampus.

In addition to the exclusionary criteria described above, participants in the CBV study were required to weigh less than 200 pounds, be aged 18 years or older, and pass a kidney function screening. Twenty-five patients (56% of sample) were excluded at the CBV data acquisition stage for the following reasons: 9 patients were determined to be ineligible upon further screening (excluded for weight=6; age=2; medical condition=1); 10 declined to participate; 2 gained weight between screening and scanning; 1 due to illness duration; and data was not acquired on 3 patients due to equipment or IV placement failure. We acquired and analyzed data in 20 of the 45 patients and 31 of the 35 controls included in the fMRI data analysis. Despite the difference in sample size between the fMRI and CBV cohorts, the only difference in demographic or clinical characteristics between the two samples was that patients who underwent both CBV and fMRI had a slightly higher score on the PANSS positive subscale (Table S1).

Task fMRI

Task design

Participants completed a single run of a block design 1-back task taken from a fusiform face area localizer (6) and was composed of 9 blocks of 16 scene, face, or scrambled images using E-Prime software, version 2 (Psychology Software Tools, Pittsburgh, PA). Block order was consistent across participants, but specific images within blocks were pseudorandomized for each participant. Each block consisted of 16 images presented for 750ms each followed by a 250ms fixation period and blocks were separated by fixation periods (5-16s). Participants were

instructed to respond by button-press if the current image matched the immediately preceding image (0-3 target matches per block). We measured performance on the 1-back task using mean hit rate, correct rejection rate, and reaction time for each condition.

Structural and functional MRI data acquisition

Imaging data was acquired on a 3T Philips Intera Achieva scanner at the Vanderbilt University Institute of Imaging Sciences (Philips Healthcare, Inc.). We obtained structural images with a 3D T1-weighted sequence (voxel size = $1mm^3$; TR = 8.0ms; TE = 3.7ms; field of view = $256mm^2$; number of slices = 170; gap=0). We collected 111 volumes of whole brain fMRI data during the task with an echo planar imaging sequence (38 ascending slices, oriented at -15° relative to the intercommissural plane; voxel size = 3.0 x 3.0 x 3.2mm; TR = 2s; TE = 28.0ms; flip angle = 90°). This acquisition protocol and sequence parameters were designed to maximize signal in the hippocampus and ventral brain regions (7).

Structural and functional MRI processing and analysis

We analyzed structural and functional data with SPM12 (http://www.fil.ion.ucl.ac.uk/spm) in Matlab 2018a (Mathworks, Inc.) using standard parameters. Functional images were realigned to the mean image. The structural image was then coregistered to the mean functional image, segmented, and normalized to MNI space. The realigned functional images were normalized by applying the deformation fields derived from structural image processing, then spatially smoothed with a 6mm full width at half-maximum Gaussian kernel. Framewise displacement of functional data for each participant was calculated using FSL's fsl_motion_outliers (http://fsl.fmrib.ox.ac.uk/fsl).

The first level analysis included separate regressors for the scene, face, and scramble conditions, modeling the onset of each image in each condition with a stimulus duration = 0,

convolved with the canonical hemodynamic response. A high-pass filter with a cutoff of 128s was applied. Because the face stimuli consisted of faces in the context of a scene background (see Figure 2A in main text for an example), rather than cropped to contain only faces, our primary analyses used the contrast estimating the difference in parameter estimates for the average response of scene and face versus scramble conditions to increase statistical power. For brevity, in the main text we refer to the average response to the scene and face conditions as "scene." Additional analyses examining the specificity of this response when limited to scene stimuli only (rather than faces) are presented in the supplement. The voxel inclusion mask from the first level analysis of each participant was overlaid onto the group mean T1 image and visually inspected for coverage of the anterior hippocampus to ensure against signal loss due to inhomogeneity artifacts.

Region of interest definition and analysis

We constructed sample-specific masks of the left and right whole, anterior, and posterior hippocampal regions for group-level region of interest analyses. Each participant's T1 structural image was processed using Freesurfer 6 with standard parameters (http://surfer.nmr.mgh.harvard.edu/; (8, 9)) and the hippocampal subfield analysis module (development version 20180220; (10)). The resulting segmentations from each participant were visually inspected for errors (inclusion of tissue outside the hippocampus, incomplete hippocampal segmentation). Hippocampal segmentations from 14 participants were excluded following this step (11 patients, 3 controls). The anterior hippocampal region of interest was defined using the Freesurfer segmentation of the hippocampal head and the posterior hippocampal region of interest was defined as the sum of the body and tail segmentations. The whole hippocampus was defined as the sum of the anterior and posterior regions of interest. The regions of interest for each participant were coregistered to the participant's mean functional image, and normalized to MNI space at the same resolution as the functional data

with nearest-neighbor interpolation using the deformation fields derived from structural image segmentation described above. We then constructed group mean whole, anterior, and posterior hippocampal regions of interest from the 110 participants whose segmentations passed quality assurance. The hippocampal masks were constructed by concatenating the regions of interest from each participant, calculating the mean across all participants, and thresholding the result at 50% overlap. The whole hippocampal masks were used for group voxelwise analyses.

Creation of activation frequency maps

To demonstrate scene activation of the anterior hippocampus at the individual level, we constructed overlap maps from the first-level analysis results of each participant based on Hodgetts et al. (11). First, the SPM t-contrast map of the difference in parameter estimates for the average response of scene and face versus scramble conditions for each individual was converted to a z-score map. This z-score map was thresholded at z=2.3 (p=.01), masked with the sample specific hippocampal region of interest described above, and binarized. For each group, we then combined the individual level maps into group activation frequency maps such that each voxel represented the number of participants with activation above a threshold of z=2.3 (main text, Figure 2B).

Cerebral blood volume (CBV) imaging

CBV data acquisition

A 3D T1 Fast Field Echo sequence (12) was used to acquire T1-weighted pre- and post-contrast images with the following parameters: TR = 20ms, TE = 3.98 ms, field-of-view = 256 x 256 mm^2, spatial resolution = 0.80 x 0.80 x 4 mm^3, slices = 30, SENSE factor = 2.5, flip angle = 25°. A power injector (Medrad®, PA, USA) was used for contrast administration (Magnevist® - Gadopentetate dimeglumine, Bayer Schering Pharma, Germany, 0.1 mmol/kg) and subsequent 40 mL saline flush through an 18G needle in the antecubital vein. After contrast administration,

post-contrast images were acquired approximately 4 minutes later. Images were acquired perpendicular to the long axis of the hippocampus. We compared the fractional increase in tissue signal after the contrast agent had thoroughly perfused the microvasculature and equilibrated in the blood.

Hippocampal segmentation for CBV data analysis

Manual segmentation of the hippocampus was completed by one rater (PT) in the native CBV space using criteria from the modified Pruessner protocol (13). The oblique-coronal series for each subject was numbered and aligned across all subjects based on the presence or absence of the uncus. From this method, three slices were labeled as anterior and three slices were labeled as posterior for the whole hippocampal formation. Due to individual differences in anatomy (e.g., a larger or smaller hippocampus), each person's hippocampus was aligned using slices 3-4 as the transition point from the anterior to posterior hippocampus for analytical purposes. Average CBV values were generated for each slice and used for statistical analyses.

CBV data processing and analysis

AFNI (14) was used to correct for subject motion in pre- and post-contrast steady state images. Absolute CBV (units = ml blood/ml parenchyma) was calculated using the following equation (12):

$$CBV = \frac{S_{\mathrm{par,post}} - S_{\mathrm{par,pre}}}{S_{\mathrm{ss,post}} - S_{\mathrm{ss,pre}}} * 100$$

where $S_{par,post} - S_{par,pre}$ is the difference between the post- and pre-contrast signal in the parenchyma and $S_{ss,post} - S_{ss,pre}$ denotes the difference between the post- and pre-contrast signal in the superior sagittal sinus. To minimize contribution from large epicortical vessels, a 10% regional CBV threshold was used (i.e., voxels with CBV values greater than 10 were excluded). The CBV maps were coregistered to the T1 structural data using FSL's FLIRT (15),

and the inverse transform was used to bring the hippocampal regions of interest into the CBV space.

Supplementary analyses and results

Behavioral data

All statistical analyses were carried out in R (R Core Team, 2018) unless otherwise specified. To examine group differences in performance on the 1-back task, we conducted separate one-way ANOVAs on hit rate, correct rejection rate, and reaction time with group as a between-subjects factor (Table S2). Performance was high in both groups (mean hit rate >= 0.95), although healthy controls were faster (p=.01) and more accurate (p=.003) than patients. Although the performance across both groups was near ceiling, the decreased accuracy and increased reaction time in patients relative to controls suggests the possibility that our findings may be related to differences in attention between the groups. The association of anterior hippocampal baseline CBV with activation during the scene processing task suggests that the observed differences in hippocampal fMRI response are not simply related to attention. However, this needs to be stringently tested in future studies, possibly by including an object-only condition where scene processing would not be required but attentional differences could be controlled for.

Exploratory whole brain fMRI analysis

In addition to the region of interest analyses described in the main text, we carried out additional whole brain analyses to confirm that activation of the hippocampus was not simply the result of activation extending from adjacent regions, such as the parahippocampal cortex. One-sample whole-brain t-tests of the average response to scenes versus scrambled images were carried

out in SPM12 separately for the healthy control and early psychosis groups and thresholded at a voxelwise familywise error<.05. These analyses confirmed the within-group region of interest findings (Supplementary Figure S1).

Association of anterior hippocampal fMRI response and CBV with clinical factors in early psychosis

We carried out additional analyses to examine whether the anterior hippocampal activation (fMRI) and CBV observed in the present study were associated with clinical characteristics of our patient sample. We conducted Spearman correlation analyses for continuous variables (PANSS scores, chlorpromazine equivalents, psychosis and prodrome duration) and Welch's t-tests for categorical variables (medication status, smoking status). We found no evidence for an association between clinical characteristics and anterior hippocampal fMRI response to scenes or with anterior hippocampal CBV, with the exception that current smokers had a higher fMRI response (Table S3). It is likely that the impact of hippocampal hyperactivity on the psychosis phenotype is multifactorial and dependent on interactions with cortical regions and intermediate cognitive processes such as memory that may vary by individual (16). For example, hippocampal hyperactivity may lead to exaggerated association of unrelated items (e.g., delusions) through impaired relational binding and inference. Future studies are needed to confirm this hypothesis.

References

1. First M, Spitzer R, Miriam G, et al.: Structured Clinical Interview for DSM-IV-TR Axis I Disorders, Research Version, Patient Edition with Psychotic Screen (SCID-I/P W/PSY SCREEN)2002;
2. Kay SR, Fiszbein A, Opler LA: The Positive and Negative Syndrome Scale (PANSS) for Schizophrenia. Schizophr Bull 1987; 13:261–276
3. Perkins DO, Leserman J, Jarskog LF, et al.: Characterizing and dating the onset of symptoms in psychotic illness: the Symptom Onset in Schizophrenia (SOS) inventory. Schizophr Res 2000; 44:1–10

4. Gardner DM, Murphy AL, O'Donnell H, et al.: International Consensus Study of Antipsychotic Dosing. Am J Psychiatry 2010; 167:686–693
5. Wechsler D: Wechsler Test of Adult Reading2001;
6. Williams LE, Blackford JU, Luksik A, et al.: Reduced habituation in patients with schizophrenia. Schizophr Res 2013; 151:124–132
7. Weiskopf N, Hutton C, Josephs O, et al.: Optimal EPI parameters for reduction of susceptibility-induced BOLD sensitivity losses: A whole-brain analysis at 3 T and 1.5 T. Neuroimage 2006; 33:493–504
8. Dale AM, Fischl B, Sereno MI: Cortical Surface-Based Analysis. Neuroimage 1999; 9:179–194
9. Fischl B, Salat DH, Busa E, et al.: Whole brain segmentation: automated labeling of neuroanatomical structures in the human brain. Neuron 2002; 33:341–55
10. Iglesias JE, Augustinack JC, Nguyen K, et al.: A computational atlas of the hippocampal formation using ex vivo, ultra-high resolution MRI: Application to adaptive segmentation of in vivo MRI. Neuroimage 2015; 115:117–137
11. Hodgetts CJ, Shine JP, Lawrence AD, et al.: Evidencing a place for the hippocampus within the core scene processing network. Hum Brain Mapp 2016; 37:3779–3794
12. Lin W, Celik A, Paczynski RP: Regional cerebral blood volume: a comparison of the dynamic imaging and the steady state methods. J Magn Reson Imaging 1999; 9:44–52
13. Woolard AA, Heckers S: Anatomical and functional correlates of human hippocampal volume asymmetry. Psychiatry Res - Neuroimaging 2012; 201:48–53
14. Cox RW: AFNI: software for analysis and visualization of functional magnetic resonance neuroimages. Comput Biomed Res 1996; 29:162–73
15. Jenkinson M, Smith S: A global optimisation method for robust affine registration of brain images. Med Image Anal 2001; 5:143–56
16. Heckers S: Neuroimaging studies of the hippocampus in schizophrenia. Hippocampus 2001; 11:520–528

Supplementary Tables

TABLE S1. Comparison of demographic and clinical characteristics for patients (total n=45) with and without CBV.

	fMRI only	CBV + fMRI
N	25	20
	Statistic	**p**
Age (yrs.)	1.29	.21
Participant Education (yrs.)	1.41	.17
Parental Education (yrs.)	-0.51	.61
WTAR	-0.48	.63
Sex (M/F)	0.56	.45
Race (W/B/O)	1.46	.48
Tobacco use (Y/N)	0.20	.65
PANSS		
Positive	-2.12	.04
Negative	-0.58	.56
General	-1.02	.31
Duration of psychosis (mos.)	-0.44	.66
Duration of prodrome (mos.)	-0.59	.56
Chlorpromazine equivalents[a]	-0.01	.99
Diagnosis	2.63	.26
Current antipsychotic treatment (Y/N)	1.28	.26

[a.]Chlorpromazine equivalents were unavailable for 1 patient with fMRI only and 1 patient with CBV + fMRI.

TABLE S2. Behavioral performance.

	Healthy Controls		Early Psychosis		Healthy Controls vs. Early Psychosis	
	Mean	**SD**	**Mean**	**SD**	**Statistic**	**p**
Hit rate	0.99	0.04	0.97	0.09	4.53	.04
Correct rejection rate	0.99	0.01	0.99	0.01	2.09	.15
RT (ms)	512.82	56.44	552.78	90.32	6.33	.01

TABLE S3. Association of clinical characteristics with anterior hippocampal fMRI and CBV response in patients.

	fMRI N=45		**CBV** N=20	
	Statistic	**p**	**Statistic**	**p**
PANSS				
Positive	0.16	.30	0.20	.34
Negative	0.10	.51	0.14	.54
General	0.04	.78	0.22	.35
Duration of psychosis (mos)	0.12	.43	-0.06	.81
Duration of prodrome (mos)	0.08	.62	-0.22	0.35
Chlorpromazine equivalents	-0.02	.92	0.19	.43
Medicated vs. Unmedicated	-0.34	.74	0.95	.38
Smokers vs. Non-smokers	3.38	.003	-0.46	.65

Supplementary Figures

FIGURE S1. Scene processing engages a network of brain regions including the hippocampus, parahippocampal, medial prefrontal, posterior cingulate/retrosplenial, inferior parietal, lateral occipital, and opercular cortices in healthy controls (**A**) and early psychosis patients (**B**). Images show the results of one-sample t-tests comparing activation in response to scenes versus scrambled images and are thresholded at whole-brain voxelwise familywise error<.05.

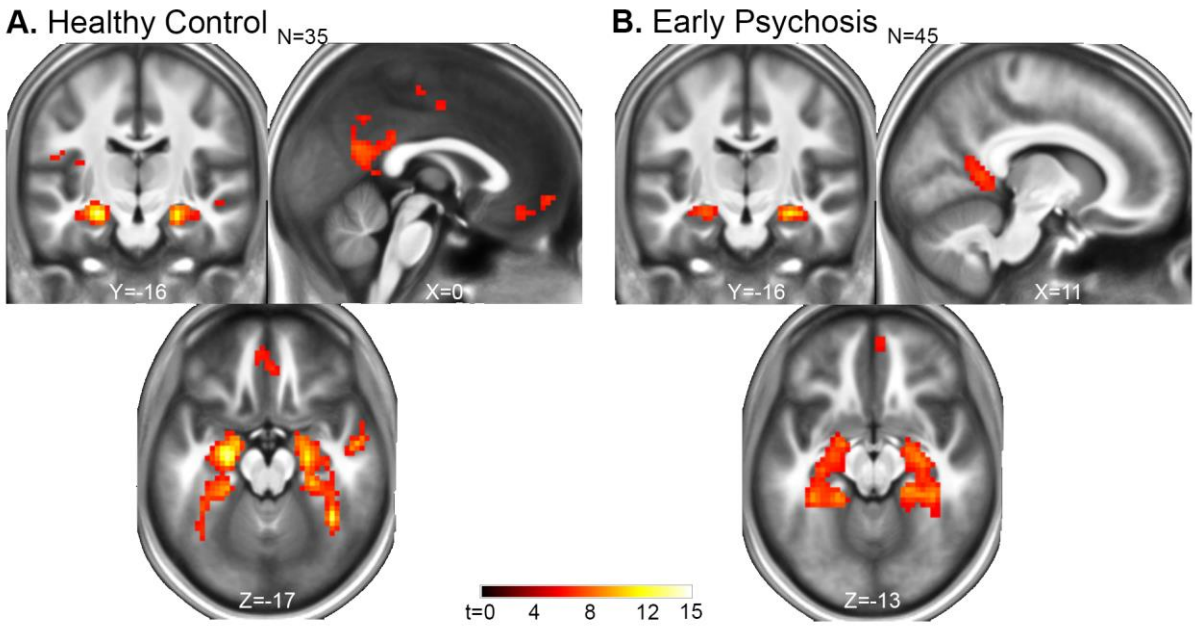

FIGURE S2. Anterior hippocampal activation in response to scenes is observable at the single subject level. This image shows activation from the contrast of scenes vs. scrambled images for a representative subject.

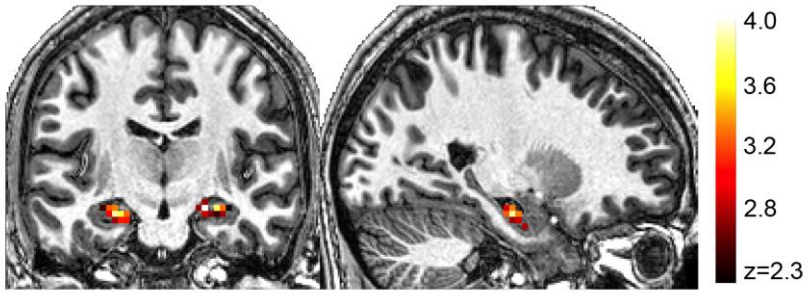

FIGURE S3. A between-group analysis examining the response to scenes only (excluding faces) versus scrambled images confirms reduced activation of the bilateral hippocampus and in early psychosis patients compared to healthy controls.